Hindawi
International Journal of Antennas and Propagation
Volume 2018, Article ID 4781465, 9 pages
https://doi.org/10.1155/2018/4781465

Research Article

A Compact Dual-Band Rectenna for GSM900 and GSM1800 Energy Harvesting

Miaowang Zeng,[1,2] **Zihong Li**,[2,3] **Andrey S. Andrenko**,[2,4] **Yanhan Zeng**,[2,5] **and Hong-Zhou Tan**[2,3]

[1]*DGUT-CNAM Institute, Dongguan University of Technology, Dongguan 523106, China*
[2]*SYSU-CMU Shunde International Joint Research Institute, Shunde 528300, China*
[3]*School of Electronics and Information Technology, Sun Yat-sen University, Guangzhou 510006, China*
[4]*eNFC Inc., Tokyo 106-0031, Japan*
[5]*School of Physics and Electronic Engineering, Guangzhou University, Guangzhou 510006, China*

Correspondence should be addressed to Yanhan Zeng; yanhanzeng@gzhu.edu.cn and Hong-Zhou Tan; tanhongzhou@sdjri.com

Received 16 February 2018; Revised 25 April 2018; Accepted 14 May 2018; Published 9 July 2018

Academic Editor: Herve Aubert

This paper presents a compact dual-band rectenna for GSM900 and GSM1800 energy harvesting. The monopole antenna consists of a longer bent Koch fractal element for GSM900 band and a shorter radiation element for GSM1800. The rectifier is composed of a multisection dual-band matching network, two rectifying branches, and filter networks. Measured peak efficiency of the proposed rectenna is 62% at 0.88 GHz 15.9 μW/cm^2 and 50% at 1.85 GHz 19.1 μW/cm^2, respectively. When the rectenna is 25 m away from a cellular base station, measurement result shows that the harvested power is able to power a batteryless LCD watch and achieve 1.275 V output voltage. The proposed rectenna is compact, efficient, low cost, and easy to fabricate, and it is suitable for RF energy harvesting and various wireless communication scenarios.

1. Introduction

As the cellular wireless communications have matured in recent years, multiband wireless signals are now widely available in the urban ambient environment. Ambient radio frequency (RF) energy harvesting has become an attractive technology since it helps various low-power devices to get rid of batteries or to improve the lifetime cycle.

A rectifying antenna (rectenna) is the most important part of RF energy harvesting system. It collects the RF signal and converts it into dc power. Some reported rectennas achieve high efficiency at single frequency, such as 2.45 GHz [1, 2]. To harvest more ambient RF energy, various dual-band rectennas [3], broadband rectennas [4, 5], and multiband rectennas [6] are reported in recent years. Several ambient RF spectrum surveys were undertaken in different countries. The surveys indicate that GSM900 and GSM1800 are the most promising bands for RF energy harvesting, rather than Wi-Fi band [7–9]. Besides, for the urban ambient RF energy harvesting, an omnidirectional antenna is preferred because the locations of RF sources are uncertain and rectenna operates in the multipath signal wave propagation environment [4].

In this paper, a dual-band rectenna is proposed at GSM900 and GSM1800 bands using monopole antenna and multisection matched rectifier. The rectenna is compact and efficient and has a higher output voltage. The rest of this paper is organized as follows. Section 2 describes the designs of antenna and rectifier, Section 3 demonstrates the simulation and measurement results, and a conclusion is drawn in Section 4.

2. Rectenna Design

The layout of the proposed dual-band rectenna is optimized and shown in Figure 1. It is composed of a dual-band

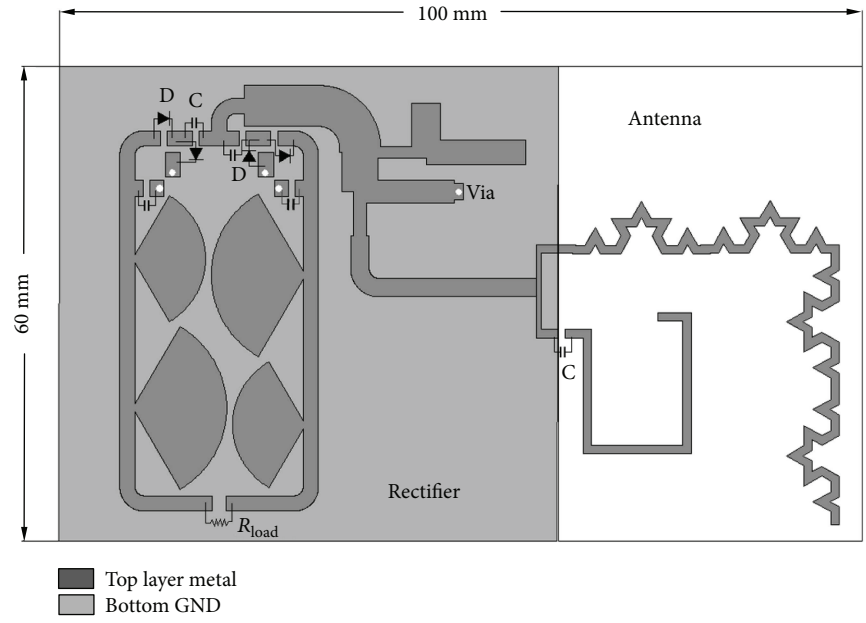

Figure 1: Layout of the proposed dual-band rectenna.

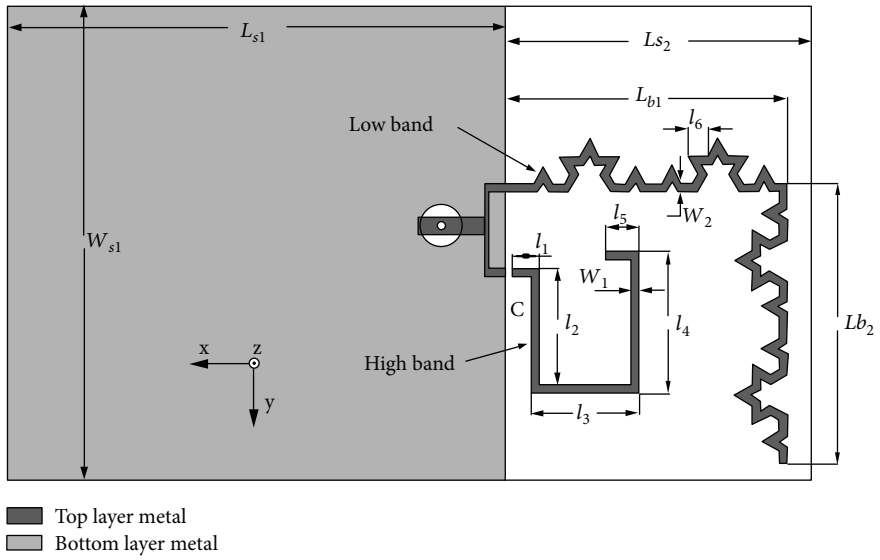

Figure 2: Layout of the proposed antenna ($w_1 = 1$, $w_2 = 1$, $l_1 = 3.2$, $l_2 = 14$, $l_3 = 13.06$, $l_4 = 17.06$, $l_5 = 4$, $l_6 = 2.43$, $c = 2$ pF, $L_{b1} = 33.85$, $L_{b2} = 33.85$, $L_{s1} = 59.83$, $L_{s2} = 36.69$, $W_{s1} = 57$; unit: mm).

monopole antenna and a dual-band microstrip rectifier circuit. The ground plane of microstrip rectifier circuit acts as the reflector of monopole antenna, which forms a conformal and miniaturized rectenna. The rectenna is fabricated on an Arlon substrate with 0.8 mm thickness, 2.55 relative dielectric constant, and 0.002 loss tangent. The antenna and rectifier circuit are on the top layer of the substrate, while the ground plane is on the bottom. The overall dimension of the proposed rectenna is about $100 \times 60 \times 0.8$ mm^3.

2.1. Antenna Design. Figure 2 shows the layout of the proposed dual-band monopole antenna. The antenna is composed of two arms for two frequency band radiation; the longer arm is designed for lower band radiation and the shorter arm is for higher band. For the longer arm of the lower band (0.87 GHz), the L-shaped strip line is processed with second-order Koch fractal geometry. It is composed of four segments of second-order Koch fractal. Compared with the monopole with straight line, the monopole antenna with fractal strip line has a wider bandwidth and more compact size.

For the shorter arm of the higher band (1.83 GHz), the strip line is bent for compactness. The two arms are connected to a T-shaped network and fed by a 50 Ω microstrip line. In order to improve the matching of 1.83 GHz band, a Murata chip capacitor is inserted in the short arm to counteract the parasitic inductance.

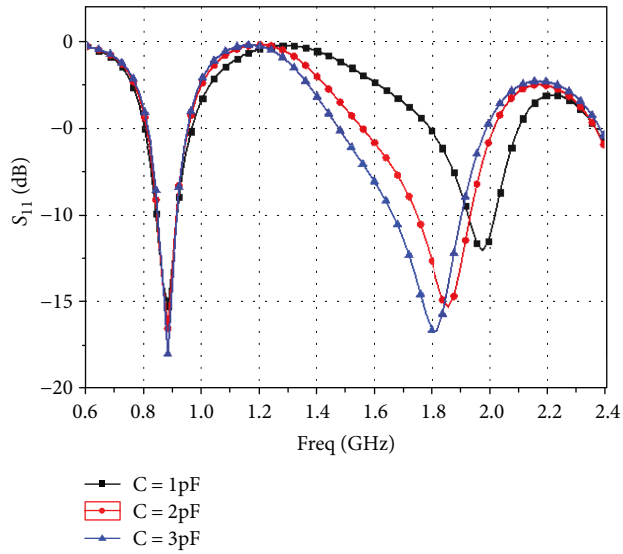

Figure 3: Simulated S_{11} of the antenna with different capacitances.

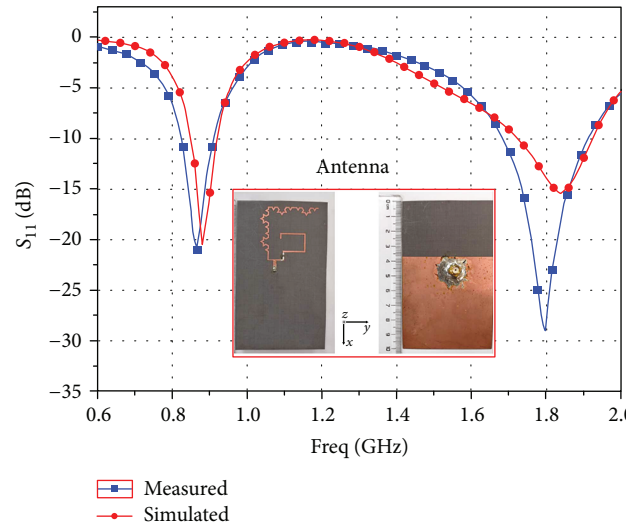

Figure 4: Simulated and measured S_{11} of the proposed dual-band Koch fractal-shaped monopole antenna.

Figure 3 shows the simulated reflection coefficient of antenna with different capacitances. We choose the value of 2 pF since its resonant frequency is 1.83 GHz.

The reflection coefficient of antenna has been measured by Keysight N5247A network analyser. Figure 4 shows the simulated and measured S_{11} and the top view photograph of the antenna. As can be seen, the antenna has two bands on 0.87 GHz and 1.8 GHz. The simulated resonant frequencies of the low band and high band are 0.88 GHz and 1.84 GHz, respectively. For the measured results, the lower resonant frequency is 0.87 GHz with S_{11} of −21 dB and the $S_{11} < -10$ dB bandwidth is from 0.83 to 0.92 GHz. The higher resonant frequency is 1.8 GHz with −29 dB reflection coefficient, and the −10 dB bandwidth is from 1.6 to 1.99 GHz. The slight frequency shift between the simulation and measurement is due to the fabrication tolerance of wet-etching technology and the parasitic parameters of chip capacitor. At lower frequency, the measured bandwidth is wider than the simulation. At high frequency, the measured S_{11} of resonant frequency is lower, and the bandwidth is wider than the simulation, which means the measured S_{11} is better than the simulation. The results indicate that the antenna is well matched at both bands. The measured bandwidth covers almost the entire bands of CDMA800, GSM900, and GSM1800 signals.

Figure 5 shows the simulated current distribution of antenna at 0.87 GHz and 1.83 GHz. At 0.87 GHz, the surface current is mainly distributed on the longer fractal arm. At 1.83 GHz, the current is concentrated on the shorter arm. It is clear that the longer arm works at the lower band, and the shorter arm radiates the higher band microwave.

The radiation characteristics have been measured in the Satimo anechoic chamber. Figure 6 depicts the simulated and measured radiation patterns of E-planes and H-planes at 0.87 GHz and 1.83 GHz, respectively. At 0.87 GHz, the H-plane is omnidirectional and the measured gain is about 0.95 dBi. At 1.83 GHz band, the measured gain is 3.15 dBi. It can be seen that the copolarization radiated field is higher than the cross-polarization field, which means the antenna is with single polarization. The cross-polarization is related to E_y-component in this case. The high-band monopole element is bent and has two sections in the y-direction. That is why the level of cross-polarization is higher at 1.83 GHz as shown in Figure 6. However, for the ambient RF energy harvesting applications, it is not a bad result as this antenna is able to receive both x-polarized and y-polarized E-field components as shown in E-plane (XOZ-plane). The radiation pattern is shown to be stable and with a broad beamwidth; thus, the antenna can receive incident microwaves from broad angle range. The total efficiencies of the antenna are 90% at 0.87 GHz and 83% at 1.83 GHz, respectively. Overall, the antenna presents a good radiation pattern at both the 0.87 GHz and 1.83 GHz bands. The H-planes show an omnidirectional pattern and the E-planes have a wide half-power beamwidth (HPBW), which is a benefit as the rectenna does not have to be aligned very precisely to operate [1].

2.2. Rectifier Design. In order to convert the GSM900/DCS1800 signals into dc power, a dual-band rectifier is proposed and designed in this section. Figure 7 shows the topology of dual-band rectifier. Full-wave Greinacher is chosen as the fundamental topology of rectifier [10, 11]. The rectifier consists of a matching network, two rectifying branches, and dc-pass filters. Each branch is a voltage doubler, and the diodes of the upper branch are in opposite polarities comparing to the lower branch. The upper branch acts as a positive doubler, and the lower branch acts as a negative doubler; thus, a positive voltage quadrupler is achieved.

Thanks to the differential output topology, the odd order components of output harmonics can be counteracted at the output. The dual-band matching network is between the input port and two rectifying branches. Thus, the dual-band signals can pass through into both two branches of rectifying networks.

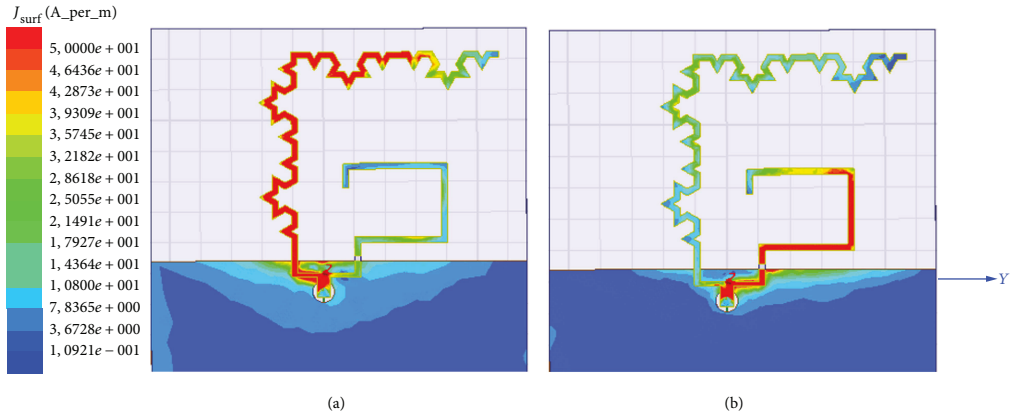

Figure 5: Current distribution of the proposed antenna at (a) 0.87 GHz, (b) 1.83 GHz.

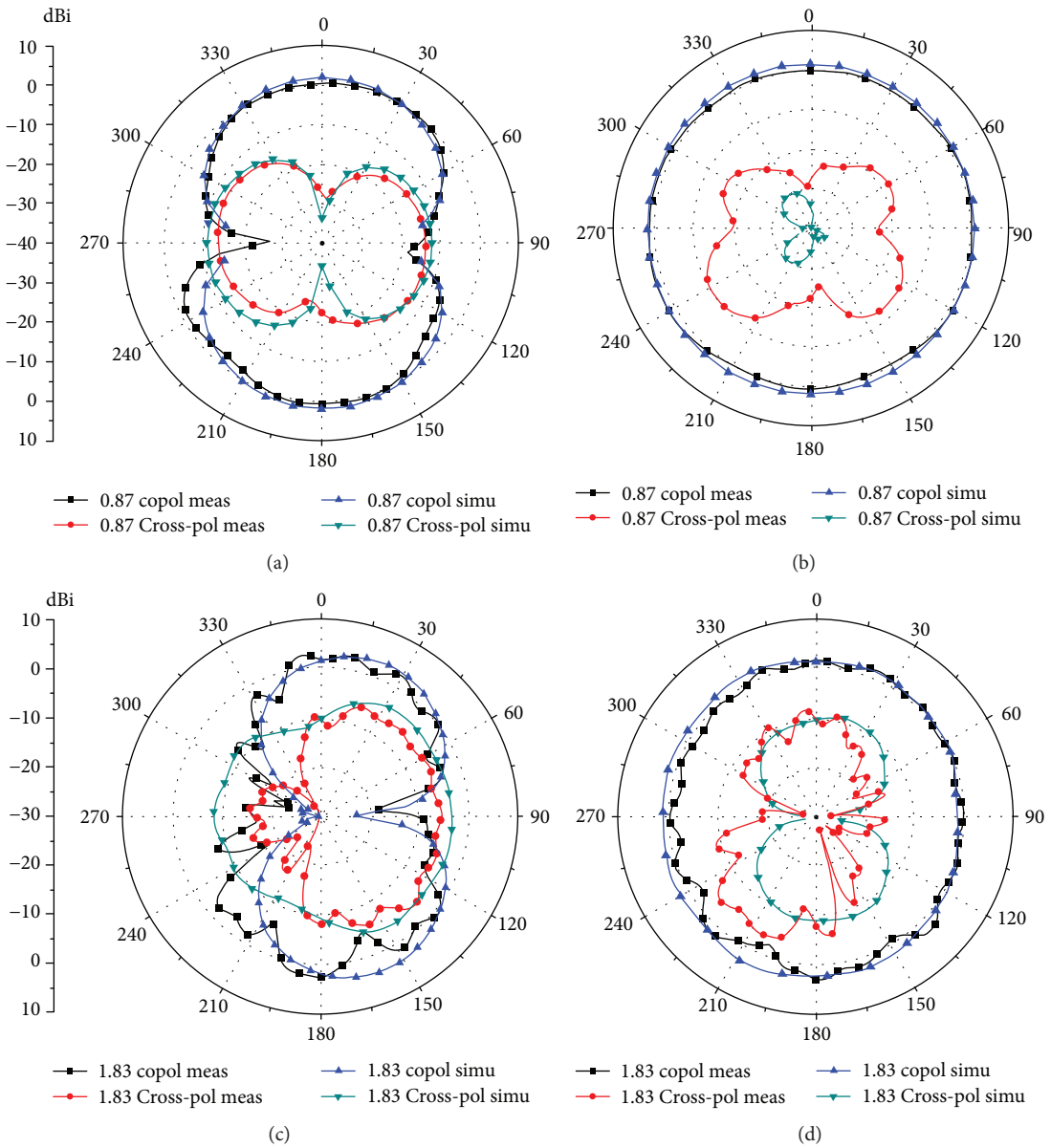

Figure 6: Simulated and measured 2D radiation pattern. (a) 0.87 GHz E-plane (XOZ-plane), (b) 0.87 GHz H-plane (YOZ-plane), (c) 1.83 GHz E-plane (XOZ-plane), (d) 1.83 GHz H-plane (YOZ-plane).

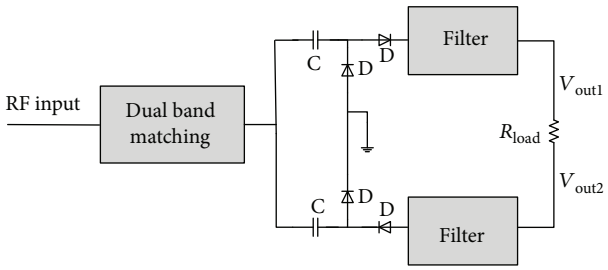

Figure 7: Topology of the proposed dual-band rectifier.

Assuming the input dual tone signal is

$$V_{in} = V_A \cos(\omega_A t + \varphi_A) + V_B \cos(\omega_B t + \varphi_B), \quad (1)$$

where ω_A and ω_B are the angular frequencies of dual tones, φ_A and φ_B are the initial phases, and V_A and V_B are the amplitudes of dual tones, respectively. The nonlinear behavior of diodes could produce rich harmonics in the rectifying process. Without counting the filter effect, since the diodes are in opposite polarities, the Fourier series of V_{out1} and V_{out2} are

$$\begin{aligned} V_{out1} &= V_{ADC} + V_{BDC} + V_{A1}\cos(\omega_A t + \varphi_A) \\ &\quad + V_{B1}\cos(\omega_B t + \varphi_B) + V_{A2}\cos(2\omega_A t + 2\varphi_A) \\ &\quad + V_{B2}\cos(2\omega_B t + 2\varphi_B)\ldots, \\ V_{out2} &= -V_{ADC} - V_{BDC} + V_{A1}\cos(\omega_A t + \varphi_A) \\ &\quad + V_{B1}\cos(\omega_B t + \varphi_B) - V_{A2}\cos(2\omega_A t + 2\varphi_A) \\ &\quad - V_{B2}\cos(2\omega_B t + 2\varphi_B)\ldots. \end{aligned} \quad (2)$$

Thus, the differential output voltage V_{out} is

$$\begin{aligned} V_{out} &= V_{out1} - V_{out2} \\ &= 2V_{ADC} + 2V_{BDC} + 2V_{A2}\cos(2\omega_A t + 2\varphi_A) \\ &\quad + 2V_{B2}\cos(2\omega_B t + 2\varphi_B)\ldots. \end{aligned} \quad (3)$$

It can be seen that only dc and even order components of harmonics exist at the differential output. The odd order components of harmonics are counteracted by the output of the branches. The dc-pass filters need only to suppress the even order harmonics and thus can be simplified.

The dual-band rectifier is designed to convert the 0.87 GHz (CDMA800/GSM900 band) and 1.83 GHz (GSM1800 band) signals into dc power. It is important to design proper filters to get a clean dc voltage and improve the rectifying efficiency [12].

The harmonic energy of output voltage is mainly distributed on the low-order harmonics, especially on the 2nd- and 4th-order harmonics. So the dc-pass filters need to suppress 1.74 GHz, 3.48 GHz, and 3.66 GHz harmonics. Figure 8 shows the optimized layout of the dual-band rectifier. The filter is composed of a 100 nF Murata chip capacitor for 1.74 GHz suppression and 10.75 mm and 8.19 mm radial stubs for 3~4 GHz harmonic suppression.

Figure 9 shows the configuration of the dual-band matching network. It is composed of multisections with several transmission lines and stubs. The first section is a shorted circuit stub for GSM1800 band matching. The second section is open stubs for GSM900 band matching. As the lower frequency has a longer conduction wavelength, it needs a larger area to satisfy the electrical length requirement. A multistub network can reduce the required area when matching for lower band and thus leads to miniaturization [13]. Finally, a modified π-shaped network with multisection and multistub is formed in Figure 9.

Schottky diode SMS7630-079LF is chosen in the rectifying circuit since it has a low threshold voltage (150 mV), which is critical for low-power energy harvesting. A spice model for the Schottky diodes provided by the Skyworks Solutions Inc. is used in the simulation [14]. The rectifier was designed and optimized in Keysight Advanced Design System (ADS) software. The rectifier is modeled in ADS based on the aforementioned rectifier topology, dc-pass filter, matching schematic, and diode model. The layout and parameters are optimized using large signal S-parameter simulator and harmonic balance simulator in ADS, as shown in Figure 8.

Figure 10 shows the simulated and measured reflection coefficient of the dual-band rectifier. The measured resonant frequencies are 0.89 GHz with −14 dB S_{11} and 1.88 GHz with −12 dB S_{11}, respectively.

The RF-dc conversion efficiency is defined as follows:

$$\text{Eff} = \frac{V_{out}^2}{P_{in} \times R_{load}} \times 100\%, \quad (4)$$

where P_{in} is the input RF power at the rectifier port, V_{out} is the output dc voltage, and R_{load} is the load resistance.

The efficiency of rectifier is measured by Keysight signal generator E8257D. Figure 11 shows the simulated and measured RF-dc efficiency against load resistance at 0 dBm input power level. It can be seen that when the load resistance varies within the 7 to 9 kΩ range, the rectifier has the highest efficiency at both frequency bands. So we have selected the 8.2 kΩ as the optimal load because such a resistor was readily available in our lab. Figure 12 shows the measured RF-dc conversion efficiency and the output dc voltage versus the input power level. For the lower band (0.89 GHz), the peak efficiency and the output voltage achieve 64% and 3.6 V at 4 dBm input power level, respectively. For the higher band (1.88 GHz), the peak efficiency and output voltage are 52% and 3.2 V at 4 dBm, respectively. The measured efficiency versus frequency is shown in Figure 13. It can be seen that the efficiencies of both bands are higher than 50% when the input power is 0 dBm.

3. Measured Results of Rectenna

Combining the antenna and rectifier, a rectenna as shown in Figure 1 is formed. The rectenna has been

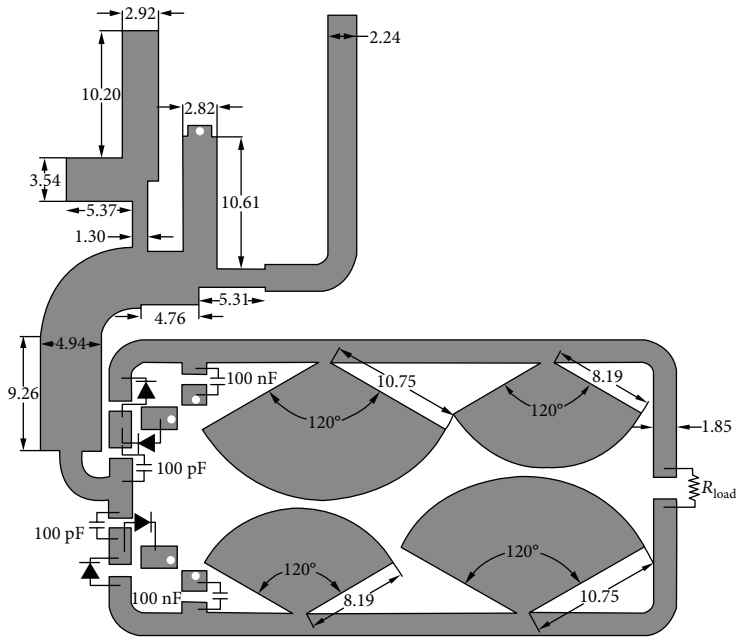

Figure 8: Layout of the proposed dual-band rectifier (unit: mm).

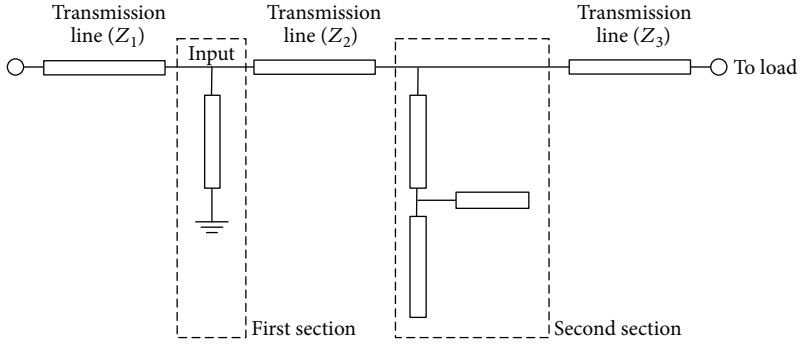

Figure 9: Configuration of the multisection dual-band matching network.

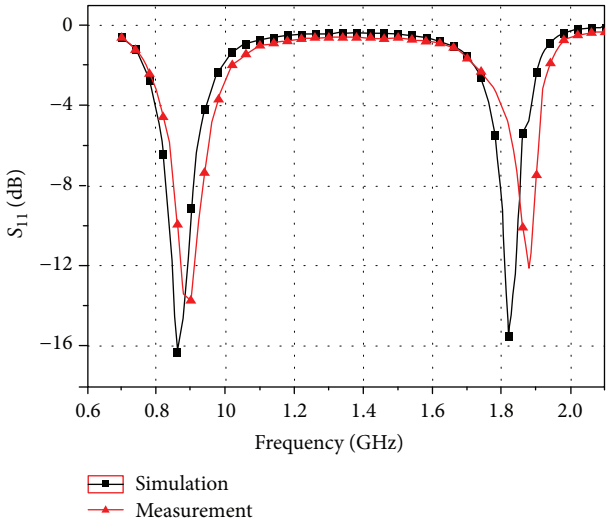

Figure 10: Simulated and measured reflection coefficient of the dual band rectifier.

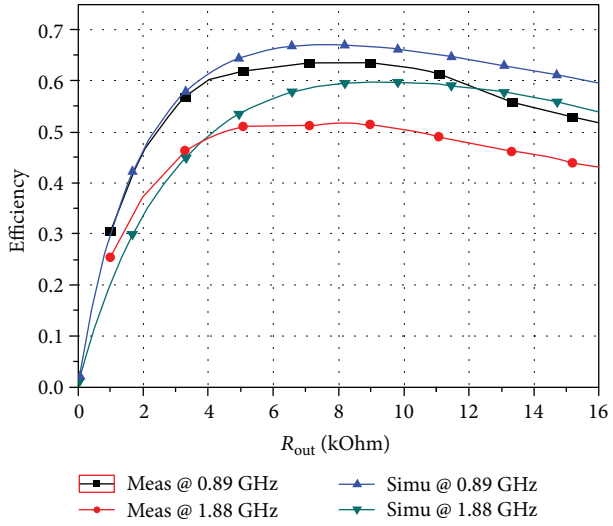

Figure 11: Simulated and measured RF-dc efficiency versus load resistance.

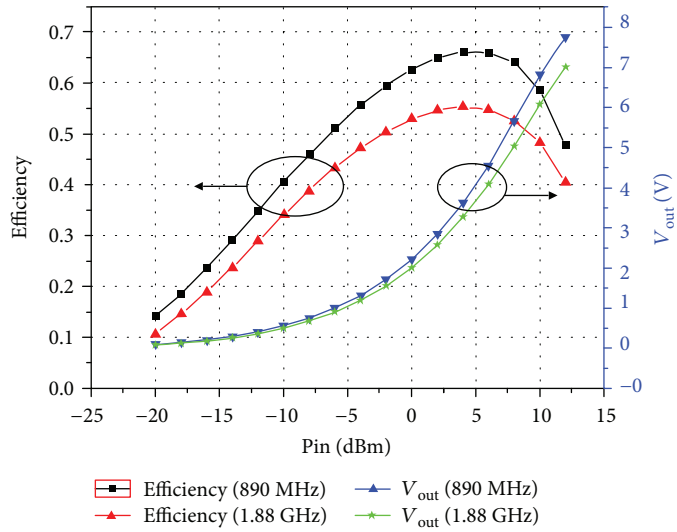

Figure 12: Measured RF-dc efficiency versus input power.

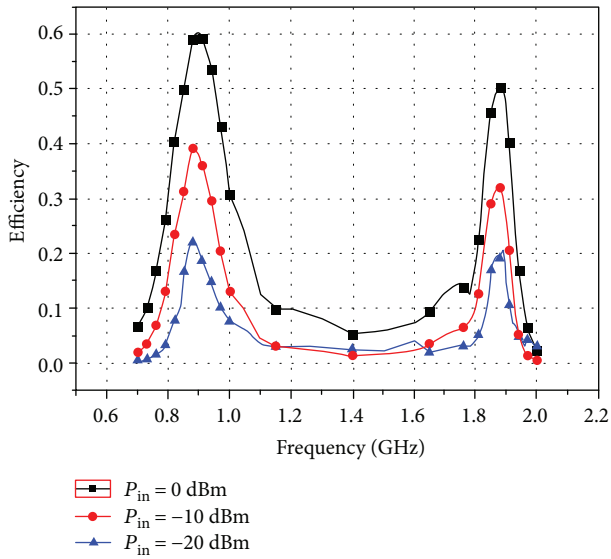

Figure 13: Measured RF-dc efficiency versus frequency.

fabricated on a 0.8 mm-thick PTFE F4B substrate with 2.55 dielectric constant. It is measured in both indoor and outdoor environment.

For indoor measurement, a signal generator (R&S SMW200A) and a standard horn antenna are used to transmit the RF power. The rectenna with 8.2 kΩ resistor is located at a distance of 1 m from transmitting antenna to satisfy far-field condition. The output dc voltage is measured by voltmeter Victor VC97.

The power density at the rectenna position is calculated by

$$\mathrm{PD} = \frac{G_T P_T}{4\pi L^2}, \tag{5}$$

where G_T is the gain of transmitting antenna, P_T is the transmitting power, and L is the distance between the transmitting antenna and the rectenna. The effective aperture of the receiving antenna is

$$A_e = \frac{G_R \lambda^2}{4\pi}, \tag{6}$$

where G_R is the gain of the proposed antenna. The received power of rectenna can be calculated using Friis transmission formula:

$$P_R = PD \cdot A_e = \frac{G_T P_T G_R \lambda^2}{(4\pi L)^2}. \tag{7}$$

And the total efficiency of the rectenna is

$$\mathrm{Eff}_{\mathrm{total}} = \frac{V_{\mathrm{out}}^2}{P_R \times R_{\mathrm{load}}} \times 100\%. \tag{8}$$

Table 1: Indoor measured results of the rectenna at 1 meter from Tx (Freq = 0.88 GHz, Tx antenna gain = 8 dBi, Rx antenna gain = 0.95 dBi).

Tx power (dBm)	Power density (μW/cm^2)	Rx power (dBm)	V_{out} (V) (8.2 kΩ load)	Eff (%)
15	1.59	−7.4	0.87	50
20	5.02	−2.4	1.67	59
25	15.9	2.6	3.04	62
27	25.2	4.6	3.72	58

Table 1 shows the indoor measurement results of the rectenna at the lower band (0.88 GHz). The gain of the transmitting antenna and receiving antenna is 8 dBi and 0.95 dBi, respectively. The distance between the two antennas is 1 meter. Using formulas (5), (7), and (8), the incident power density, received RF power, and efficiency of the rectenna against the transmitting power are calculated and shown in Table 1. When the transmitting power is 25 dBm, a peak efficiency of 62% and 3.04 V output dc voltage are achieved at 8.2 kΩ load resistance. Table 2 shows the higher

Table 2: Indoor measured results of the rectenna at 1 meter from Tx (Freq = 1.85 GHz, Tx antenna gain = 8.8 dBi, Rx antenna gain = 3.15 dBi).

Tx power (dBm)	Power density (μW/cm^2)	Rx power (dBm)	V_{out} (V) (8.2 kΩ load)	Eff (%)
15	1.91	−10.8	0.45	30
20	6.04	−5.8	1.01	47
25	19.1	−0.83	1.84	50
27	30.3	1.16	2.27	48

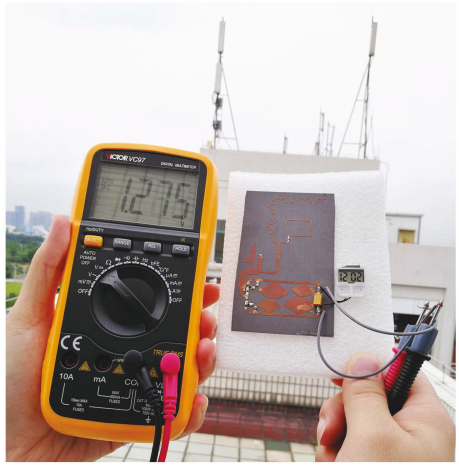

Figure 14: Rectenna outdoor measurement at about 25 meters from cellular base station.

band (1.85 GHz) measurement results. A peak efficiency of 50% and 1.84 V output dc voltage are achieved at 1 m distance from the 25 dBm transmitting source.

For outdoor experiment, the rectenna is measured at about 25 meters away from cellular base station. Figure 14 shows the setup of outdoor measurement. The load resistor is replaced with a 330 μF capacitor to store the harvested RF energy. A batteryless LCD watch and a voltmeter are connected to the output of the rectenna. The rectenna is able to harvest GSM900 and GSM1800 energy. It successfully powers up the batteryless LCD watch and outputs 1.275 V dc voltage.

Table 3 illustrates the comparison with recently reported rectennas. Among these literatures, the rectenna in this work has a higher efficiency at lower power condition, lower fabrication cost, and smaller layout size. A better overall performance is achieved in our design.

4. Conclusion

In this paper, a compact dual-band rectenna for GSM900 and GSM1800 energy harvesting has been presented and discussed. The measured total efficiency of the rectenna achieves 62% at 0.88 GHz for 15.9 μW/cm^2 power density and 50% at 1.85 GHz for 19.1 μW/cm^2 power density, respectively. The proposed rectenna is compact and easy to fabricate, which can be used in various RF energy harvesting and wireless communication applications.

Table 3: Comparison with recently reported rectennas.

Ref.	Freq (GHz)	Dimension (mm^3)	Fabrication complexity	Peak Eff @ power density (μW/cm^2)
[2]	2.45	110 × 100 × 4.7	Medium, 3 layers PCB	63% @ 525
[4]	0.98 1.8	100 × 90 × 0.8	Easy, 2 layers PCB	60.4% @ 44 17% @ 157
[15]	0.915 2.45	60 × 60 × 30	Difficult, 3D PCB	48% @ 7.6 39% @ 32
This work	0.88 1.85	100 × 60 × 0.8	Easy, 2 layers PCB	62% @ 15.9 50% @ 19.1

Data Availability

The data used to support the findings of this study are available from the corresponding author upon request.

Conflicts of Interest

The authors declare that they have no conflicts of interest.

Acknowledgments

This work was supported by the National Natural Science Foundation of China (Grant nos. 61704037 and 61473322), the Natural Science Foundation of Guangdong Province (Grant no. 2017A030310655), and the Science and Technology Project of Guangzhou (Grant no. 201804010464).

References

[1] H. Sun, Y.-x. Guo, M. He, and Z. Zhong, "Design of a high-efficiency 2.45-GHz rectenna for low-input-power energy harvesting," *IEEE Antennas and Wireless Propagation Letters*, vol. 11, pp. 929–932, 2012.

[2] Z. Harouni, L. Cirio, L. Osman, A. Gharsallah, and O. Picon, "A dual circularly polarized 2.45-GHz rectenna for wireless power transmission," *IEEE Antennas and Wireless Propagation Letters*, vol. 10, pp. 306–309, 2011.

[3] H. Sun, Y. X. Guo, M. He, and Z. Zhong, "A dual-band rectenna using broadband Yagi antenna array for ambient RF power harvesting," *IEEE Antennas and Wireless Propagation Letters*, vol. 12, pp. 918–921, 2013.

[4] M. Arrawatia, M. Baghini, and G. Kumar, "Broadband bent triangular omnidirectional antenna for RF energy harvesting," *IEEE Antennas and Wireless Propagation Letters*, vol. 15, pp. 36–39, 2015.

[5] C. Song, Y. Huang, J. Zhou, J. Zhang, S. Yuan, and P. Carter, "A high-efficiency broadband rectenna for ambient wireless energy harvesting," *IEEE Transactions on Antennas and Propagation*, vol. 63, no. 8, pp. 3486–3495, 2015.

[6] C. Song, Y. Huang, P. Carter et al., "A novel six-band dual CP rectenna using improved impedance matching technique for ambient RF energy harvesting," *IEEE Transactions on Antennas and Propagation*, vol. 64, no. 7, pp. 3160–3171, 2016.

[7] M. Piñuela, P. D. Mitcheson, and S. Lucyszyn, "Ambient RF energy harvesting in urban and semi-urban environments," *IEEE Transactions on Microwave Theory and Techniques*, vol. 61, no. 7, pp. 2715–2726, 2013.

[8] A. S. Andrenko, X. Lin, and M. Zeng, "Outdoor RF spectral survey: a roadmap for ambient RF energy harvesting," in *TENCON 2015 - 2015 IEEE Region 10 Conference*, pp. 1–4, Macao, China, 2015.

[9] H. J. Visser, A. C. F. Reniers, and J. A. C. Theeuwes, "Ambient RF energy scavenging: GSM and WLAN power density measurements," in *2008 38th European Microwave Conference*, pp. 721–724, Amsterdam, Netherlands, 2008.

[10] U. Olgun, J. L. Volakis, and C.-C. Chen, "Design of an efficient ambient WiFi energy harvesting system," *IET Microwaves, Antennas & Propagation*, vol. 6, no. 11, pp. 1200–1206, 2012.

[11] C. R. Valenta and G. D. Durgin, "Harvesting wireless power: survey of energy-harvester conversion efficiency in far-field, wireless power transfer systems," *IEEE Microwave Magazine*, vol. 15, no. 4, pp. 108–120, 2014.

[12] T. W. Yoo and K. Chang, "Theoretical and experimental development of 10 and 35 GHz rectennas," *IEEE Transactions on Microwave Theory and Techniques*, vol. 40, no. 6, pp. 1259–1266, 1992.

[13] A. Fukuda, H. Okazaki, S. Narahashi, and T. Nojima, "Concurrent multi-band power amplifier employing multi-section impedance transformer," in *2011 IEEE Topical Conference on Power Amplifiers for Wireless and Radio Applications*, pp. 37–40, Phoenix, AZ, USA, 2011.

[14] *Surface Mount Mixer and Detector Schottky Diodes, Data sheet*, Skyworks Solutions, Inc., 2013.

[15] K. Niotaki, S. Kim, S. Jeong, A. Collado, A. Georgiadis, and M. M. Tentzeris, "A compact dual-band rectenna using slot-loaded dual band folded dipole antenna," *IEEE Antennas and Wireless Propagation Letters*, vol. 12, pp. 1634–1637, 2013.